3 Biotech (2025) 15:408
https://doi.org/10.1007/s13205-025-04572-3

ORIGINAL ARTICLE

Application of nanoparticles as biostimulator for growth of *Digitalis ferruginea* subsp. *ferruginea L.* under in vitro conditions

Dipul Kumar Biswas[1,3] · Özge Kaya[3] · Ömer Can Ünüvar[3] · Mehmet Örgeç[3] · Sandeep Kumar Verma[1] · İlknur Dağ[4,5] · Mehmet Doğan[6] · Buhara Yücesan[7] · Muhammad Sameeullah[8,9] · Songül Gürel[2,3] · Ekrem Gürel[2,3]

Received: 14 May 2025 / Accepted: 6 October 2025 / Published online: 31 October 2025

Abstract

This study examined the physiological, biochemical, ultrastructural, and cytological effects of zinc (Zn), copper (Cu), zinc oxide (ZnO), copper oxide (CuO), and titanium dioxide (TiO_2) nanoparticles (NPs) on *Digitalis ferruginea* subsp. *ferruginea* L. under in vitro conditions. Germination, stomatal conductance, photosynthetic rate, chlorophyll and carotenoid content, anatomical structures and cytotoxicity were analyzed. Germination percentages were not significantly affected by NP exposure ($p = 0.800$), although minor variations were measured between treatments. ZnO NPs at 20 µg/mL increased photosynthetic rate (6.85 ± 1.01 µmol m^{-2} s^{-1}), while CuO NPs at 5 µg/mL induced strong inhibitory effects (0.79 ± 0.45 µmol m^{-2} s^{-1}). CuO NPs at 7.5 µg/mL significantly reduced chlorophyll a and b contents ($p < 0.001$), and CuO at 2.5 µg/mL caused a decrease in stomatal conductance ($p = 0.009$). TEM analysis showed that lower NP concentrations preserved cell wall and chloroplast integrity, while higher doses caused thylakoid disorganization, mitochondrial swelling, and vacuolization. Cytological observations presented that CuO, TiO_2, and high ZnO concentrations triggered chromosomal abnormalities, such as anaphase bridges, spindle disturbances, and chromosome fragmentation. Root viability assays confirmed the membrane damage in CuO 2.5 µg/mL ($p < 0.001$), while ZnO 20 µg/mL retained integrity. In conclusion, NP effects on *Digitalis ferruginea* subsp. *ferruginea* L. were dose- and type-dependent, with ZnO NPs exhibiting biostimulant properties at optimal concentrations and CuO NPs demonstrating cyto- and genotoxic effects. These findings point out the dual role of NPs as growth promoters and stress inducers, emphasizing the importance of NP exposure in plant biotechnological applications.

Keywords Metal nanoparticles · Metal oxide nanoparticles · Plant physiology · *Digitalis ferruginea* subsp. *ferruginea* L. · Photosynthesis · TEM

Introduction

Nanotechnology is a rapidly advancing field in modern materials science, offering novel possibilities in various disciplines. Nanoparticles (NPs) and nanomaterials (NMs) possess unique physicochemical characteristics due to their nanoscale dimensions, typically defined as having at least one dimension below 100 nm (Asha et al. 2016; Rastogi et al. 2017; Khan 2020; Baig et al. 2021). These properties—such as size, shape, composition, surface chemistry, and stability—affect how NPs interact with biological systems and determine their potential applications. Advances in nanotechnology have led to its integration into diverse areas, including natural sciences, engineering, electronics, medicine, and agriculture. In plant sciences, nanotechnology has been explored for enhancing seed germination, promoting growth, and modulating secondary metabolite production.

Digitalis ferruginea subsp. *ferruginea* L., commonly known as rusty foxglove, is a member of the Plantaginaceae family and is native to regions such as Hungary, Romania, Türkiye, the Balkans, Italy, Lebanon, and the Caucasus (Davis et al. 1988; Verma et al. 2016). This biennial or short-lived perennial grows up to 1.2 m in height, forming a rosette of dark green leaves and producing spikes of russet, tubular flowers in summer. In Türkiye, it is found mainly in forested areas, scrublands, and rocky terrains (Eker et al. 2016; Verma et al. 2012). Its leaves contain cardenolide derivatives with strong cardiotonic effects, making it an important medicinal species used in the treatment of heart diseases.

Extended author information available on the last page of the article

NP-plant interactions are influenced by several factors, including particle size, chemical composition, morphology, surface characteristics, stability in suspension, and the synthesis method employed (Da Costa and Sharma 2016; Wang et al. 2016; Teske and Detweiler 2015). Depending on these parameters, NPs can exert beneficial effects—such as enhanced nutrient uptake and growth stimulation—or cause phytotoxicity. Recent studies have advanced our understanding of NP effects on plant physiology, particularly under stress conditions. For example, green-synthesized ZnO NPs improved drought resilience in pepper by enhancing stomatal function and boosting photosynthesis, likely via upregulated H^+-ATPase activity and phytohormone modulation (Guzel Deger et al. 2025). In another study, it was reported that CuO NPs promoted growth in soybean at 100 ppm and in chickpea at 60 ppm, while higher concentrations inhibited growth. ZnO NPs supported full seed germination at 100–200 mg/L, while TiO_2 NPs had beneficial effects on *Cicer arietinum* and forage crops but were also linked to delayed germination at elevated concentrations (Karale et al. 2025; Stałanowska et al. 2023).

This study aims to evaluate the physiological, biochemical, and cytological effects of copper (Cu), copper oxide (CuO), zinc (Zn), zinc oxide (ZnO), and titanium dioxide (TiO_2) nanoparticles on *D. ferruginea* subsp. *ferruginea* L. under in vitro conditions, at varying concentrations, to identify both their potential as biostimulants and their possible toxic effects.

Materials and methods

Plant and nanoparticles

The seeds of *D. ferruginea* subsp. *ferruginea* L. were collected from Bolu, Türkiye, situated at an elevation of 1334 m, with coordinates around 40°36.02′N and 31°16.36′E, in September 2008. Species identification was applied following the protocols defined by Davis et al. (1988). The seeds were cultivated in vitro in Murashige & Skoog (MS) medium enriched with vitamins (M0222), supplied from Duchefa Biochemie B.V., Netherlands.

NPs used in the study; Zn (CAS Number: 7440-66-6); ZnO (CAS Number: 1314-13-2); Cu (CAS Number: 7440-50-8); CuO (CAS Number: 1317-38-0); and TiO_2 (CAS Number: 13463-67-7) were obtained from Sigma Chemical Company (St. Louis, MO, USA). The NPs were characterized using transmission electron microscopy (TEM), scanning electron microscopy (SEM), X-ray diffraction (XRD), Fourier-transform infrared spectroscopy (FTIR), and dynamic light scattering (DLS).

Application of NPs and their impacts on plant biochemical and physiological parameters

Concentrates of NPs (0, 5.0, 10.0, 15.0, and 20.0 µg/mL for Zn, ZnO, and TiO_2 NPs and 0, 1.25, 2.50, 5.0, and 7.5 µg/mL for Cu and CuO) were prepared using ddH_2O, then stabilized through ultrasonication for uniform dispersion and reduced aggregation in subsequent experiments. The seeds were sterilized by immersing in 5 mL of 100% commercial bleach in a 50 mL tube, mixing, and transferring to a 250 mL beaker. The bleach concentration was adjusted to 5% with sterile dH_2O, and the mixture was stirred at 250 rpm on a stirrer for 40 min (Verma et al. 2014). Subsequently, the seeds were immersed in solutions with various concentrations of Zn, ZnO, TiO_2, Cu and CuO NPs, which are indicated above for 24 h. Cu and CuO were used at lower concentrations because of their higher toxicity. For control, seeds were exposed only to dH_2O for one day (24 h). Germination of seeds was carried out on MS (Murashige and Skoog 1962) medium containing NPs at relevant concentrations.

Germination of the seeds and determination of the effects of NPs on germination

Germination was conducted under dark conditions at 23.0 ± 1.0 °C for 10 days. The primed seeds were placed in Petri dishes and incubated for 4 weeks in a germination chamber under a 16 h light–8 h dark period with fluorescent light (50 µmol m^{-2} s^{-1}). The humidity of the chamber was maintained at 55–60%. The percentages of the germinations were calculated (germinated seeds/total seeds) × 100) (Verma et al. 2014; Yücesan et al. 2016; Verma et al. 2018a, b).

Investigation of changes in stomata and trichomes due to NP exposure

The measurements of stomatal dimensions were performed using transparent sealing tape. Specimens were taken from the lower epidermal layer around the midrib of the youngest 3rd leaves from 9-week-old plants (Verma et al. 2018a, b). The samples of the stomata and trichomes were analyzed with a light microscope (BX51, Olympus, Japan). Stomata and trichome lengths and stomatal widths in micrometers µm, and the number of stomata per 1 cm^2 were analyzed from the photographs using ImageJ software (Schneider et al. 2012).

Obtaining photosynthetic rate and stomatal conductivity measurements

Photosynthetic rate and stomatal conductivity were measured on leaves of the 9-week-old seedlings treated with NPs and compared to control leaves using LI-6800 Portable

Photosynthesis System (LI-COR Inc. Lincoln, USA) (Willis and Balasubramaniam 1968).

Determination of the chlorophyll and carotenoids contents

Chlorophyll a (Ch a), chlorophyll b (Ch b), and carotenoids were measured using the procedure described by Lichtenthaler and Wellburn, (1983). Following that, the equations were used to determine the chlorophyll and carotenoids contents;

$$\text{Chl a} = \left(3.95 \times A_{665}\right) - (6.88 \times A_{649})$$

$$\text{Chl b} = \left(24.96 \times A_{649}\right) - \left(7.32 \times A_{665}\right)$$

$$\text{Carotenoids (Chlx+c)} = \frac{1000 \text{ x A470 - 2.05 x Chla - 114.8 x Chlb}}{245}$$

Anatomical, ultrastructural and cytological studies

In the study, TEM was used to examine the ultrastructural changes in the samples tested under the lowest and highest NP concentrations. Samples were collected from 15-week-old plants, specifically from the middle of the youngest 3rd leaves, 2 mm^2 from the region adjacent to the midrib. These samples were fixed in 0.1 M phosphate-buffered saline (PBS) containing 2.5% glutaraldehyde for 2 h. Following primary fixation, the samples, washed with PBS, underwent secondary fixation for 1 h in a 0.2 M PBS containing 1% osmium tetroxide. The specimens were washed with PBS and dehydrated by a series of concentrations of ethanol (50%, 70%, 96%, and 100%). Subsequently, the samples were embedded in epoxy resin (Araldite CY212) and polymerized at 60 °C for 48 h. Using an ultramicrotome (Leica EM UC6, Germany), 60 nm thick ultrathin sections were taken from the blocks and placed on copper grids. The specimens were stained by uranyl acetate-lead citrate, dried, and analyzed using TEM (Hitachi HT7800, Japan) (Hülskamp et al. 2010).

The root tips (meristematic zone) were prepared for cytological studies of chromosomes. 9-week-old plants' roots were cleaned with dH_2O, then immersed in the fixative solution of ethanol and glacial acetic acid (3:1), and kept at 4 °C, overnight (Ma and Kabir 1992). They were hydrolyzed in HCl (1 M), stained with aceto-orcein for 2 h, and pressed onto slides for observation under a light microscope to visualize chromosomes.

Determining of root cell viability

Evans blue staining protocol was used to determine the viability of 9-week-old plant root cells. (Tamás et al. 2004). Spectrophotometric studies at 600 nm wavelength were performed to quantify cell viabilities (Vijayaraghavareddy et al. 2017; Yamamoto et al. 2001; Jacyn Baker and Mock 1994).

Statistical analysis

The data were analyzed via one-way ANOVA and compared using the Tukey's test, with results expressed as "mean ± standard deviations". The lines on the graphs show standard deviations and lower case letters (a, b, c etc.) indicate statistical differences.

Results

Characteristics of nanoparticles

TEM was employed for the structural analysis of NPs. The results are presented in Supplementary material 1. From the TEM images, the particle sizes were measured as: 19–45 nm for Cu, 112–143 nm for CuO, 19 nm for Zn, 17–24 nm for ZnO, and 15–28 nm for TiO_2. SEM was used to analyze the surface morphologies (Supplementary material 2). It was found that they displayed a uniform distribution. The XRD results of NPs were analyzed, aligning with International Centre for Diffraction Data (ICDD) reference standards (Iwashita 2016). The sizes of each NP were determined using the Debye–Scherrer equation. For Cu NPs, the peaks corresponded to ICDD card 4–0836, with a crystalline size of 37.23 nm (Supplementary material 3 A). CuO NPs displayed peaks in parallel with ICDD card 45–0937, and 20.66 nm crystalline size was calculated (Supplementary material 3B). Zn NPs exhibited peaks that matched ICDD card 4–0831, with 21.26 nm crystalline size (Supplementary material 3 C). ZnO NPs showed peaks corresponding to ICDD card 45–0937, with 14.81 nm crystalline size (Supplementary material 3D). TiO_2 NPs displayed peaks that corresponded to ICDD card 4–0831, with 48.01 nm crystalline size (Supplementary material 3E). To examine the range of chemical bonds within metal oxide-NPs, FTIR measurements were applied. The findings revealed distinct peaks (Supplementary material 4) consistent with the literature. The peaks in the FTIR spectra indicate stretching vibrations of the M–O bonds, which are highlighted by blue lines. The outcomes of DLS measurements are illustrated in Supplementary material 5, indicating the sizes as 27.0, 130.0, 59.0, 204.0, and 348.0 nm for Cu, CuO, Zn, ZnO, and TiO_2, respectively. The large particles observed with DLS may result from partial agglomeration of NPs.

The effects of NPs on germination of *D. ferruginea* subsp. *ferruginea* L.

The lowest germination percentage was recorded in Cu 1.25 µg/mL (33.34%) and Zn 5.00 µg/mL (29.36%) applications. In ZnO 5.00 µg/mL (42.04%) and Cu 5.00 µg/mL (43.00%) groups, germination percentages were close to the control group (Fig. 1). Although the germination percentage of *D. ferruginea* subsp. *ferruginea* L. varied depending on the type and concentration of NPs; these differences were not statistically significant ($p = 0.800$).

Changes in stomata and trichomes due to nanoparticle exposure

Stoma length was measured as the highest value with CuO 7.50 µg/mL (139.16 ± 9.01 µm), while TiO_2 exposure showed the lowest value with 5.00 µg/mL (103.04 ± 6.46 µm) ($p < 0.001$). When stomatal widths were examined, no significant change was observed between the groups ($p = 0.148$). On the other hand, stoma density changed significantly ($p < 0.001$), with ZnO showing the highest value at 15.00 µg/mL (609.3 ± 19.7 amount/mm^2). This finding indicates that ZnO may promote stomatal development. Significant changes were noted in terms of trichome length and density depending the types and concentrations of NPs ($p < 0.001$). While exposure of Zn NP with 20.00 µg/mL (12.67 ± 4.04 amount/mm) increased trichome density, CuO NP with 2.50 µg/mL (4.40 ± 0.69 amount/mm) showed the lowest value (Table 1).

The impacts of nanoparticles on the photosynthetic rate and stomatal conductivity

The photosynthetic rates were significantly affected by NP exposure ($p < 0.001$). The highest value was determined with ZnO 20.00 µg/mL (6.85 ± 1.01 µmol $m^{-2}.s^{-1}$), while the lowest value was reached with CuO 5.00 µg/mL (0.79 ± 0.45 µmol $m^{-2}.s^{-1}$). Statistically significant differences were also found between stomatal conductance values ($p = 0.009$), with CuO 2.50 µg/mL (0.70 ± 0.77 mol $m^{-2}.s^{-1}$) presenting the lowest conductance (Fig. 2).

The effects of nanoparticles on chlorophyll and carotenoid pigments

While the chlorophyll a level remained close to the control group in the 15.00 µg/mL of Zn (12.86 ± 4.10 µg/mL) and 5.00 µg/mL of TiO_2 (12.94 ± 3.09 µg/mL) groups, 7.50 µg/mL of CuO (6.08 ± 4.14 µg/mL) had the lowest value ($p < 0.001$). For chlorophyll b, the Zn and TiO_2 groups were found at similar levels to the control ($p = 0.004$), while CuO had the lowest values. The carotenoid concentration exhibited no significant changes between the groups ($p = 0.066$) (Table 2).

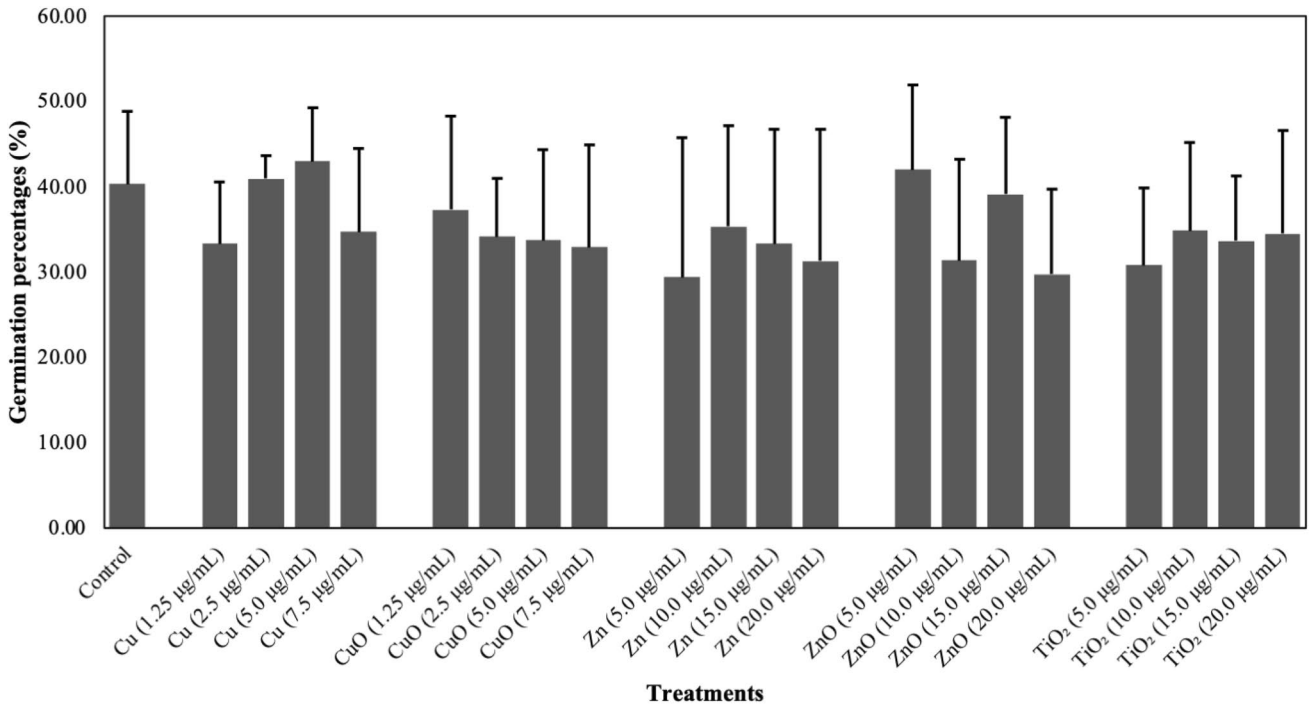

Fig. 1 The changes in the germination percentages of *D. ferruginea* subsp. *ferruginea* L.

Table 1 Changes in stomata and trichomes properties of *D. ferruginea* subsp. *ferruginea* L. leaves (Different superscript letters within a column represent significant differences according to one-way ANOVA followed by Tukey's test ($p \leq 0.05$). Groups without letters are not significantly different)

Treatments		Measurement parameters				
Nanoparticles (NPs)	Exposure concentration (µg/mL)	Stoma length (µm)	Stoma width (µm)	Stoma density (amount/mm^2)	Trichome length (mm)	Trichome density (amount/mm)
Control (w/o) NPs	–	131.83 ± 10.20^{ab}	105.73 ± 20.38	533.3 ± 50.3^{abcd}	1.98 ± 0.67^{abcde}	9.07 ± 3.44^{abc}
Cu	1.25	120.78 ± 17.95^{bc}	102.65 ± 19.47	196.0 ± 22.3^{j}	1.54 ± 0.42^{cde}	5.53 ± 1.33^{c}
	2.50	120.67 ± 10.22^{bc}	107.73 ± 43.15	465.3 ± 52.2^{cdefg}	1.79 ± 0.30^{bcde}	7.93 ± 2.69^{abc}
	5.00	124.77 ± 12.65^{ab}	119.02 ± 34.09	393.3 ± 22.0^{fgh}	2.14 ± 0.26^{abc}	8.60 ± 0.35^{abc}
	7.50	123.52 ± 7.89^{ab}	99.30 ± 25.66	440.0 ± 24.0^{defg}	1.27 ± 0.17^{e}	9.80 ± 2.31^{abc}
CuO	1.25	127.29 ± 16.97^{ab}	122.57 ± 11.94	520.0 ± 36.0^{abcde}	1.80 ± 0.40^{bcde}	5.40 ± 0.35^{c}
	2.50	122.79 ± 7.57^{b}	111.27 ± 28.42	528.0 ± 21.2^{abcde}	2.54 ± 0.65^{a}	4.40 ± 0.69^{c}
	5.00	120.34 ± 18.05^{bc}	102.00 ± 34.20	580.0 ± 8.0^{ab}	2.13 ± 0.34^{abc}	$8.67 \pm 0.61ab^{c}$
	7.50	139.16 ± 9.01^{a}	114.97 ± 27.61	381.3 ± 36.3^{fgh}	1.34 ± 0.21^{de}	9.27 ± 0.64^{abc}
Zn	5.00	106.49 ± 12.34^{cd}	97.90 ± 23.58	301.3 ± 27.2^{hi}	1.54 ± 0.23^{cde}	7.07 ± 0.83^{abc}
	10.00	116.15 ± 7.97^{bcd}	102.10 ± 25.11	377.3 ± 26.6^{gh}	1.62 ± 0.13^{cde}	9.53 ± 2.20^{abc}
	15.00	118.46 ± 11.05^{bcd}	118.97 ± 16.38	545.3 ± 53.7^{abc}	1.54 ± 0.34^{cde}	10.00 ± 1.83^{abc}
	20.00	118.14 ± 6.92^{bcd}	122.85 ± 24.04	442.7 ± 28.9^{cdefg}	2.41 ± 0.38^{ab}	12.67 ± 4.04^{a}
ZnO	5.00	128.93 ± 8.89^{ab}	101.30 ± 18.17	481.3 ± 18.0^{bcdef}	1.83 ± 0.42^{abcde}	11.80 ± 4.01^{ab}
	10.00	121.88 ± 6.94^{bc}	108.08 ± 36.93	570.7 ± 60.6^{ab}	1.78 ± 0.40^{bcde}	7.20 ± 2.88^{abc}
	15.00	131.51 ± 10.50^{ab}	116.40 ± 10.47	609.3 ± 19.7^{a}	2.00 ± 0.30^{abcd}	6.73 ± 0.76^{abc}
	20.00	126.17 ± 9.91^{ab}	118.23 ± 28.94	362.7 ± 12.2^{gh}	1.82 ± 0.24^{abcde}	8.53 ± 0.23^{abc}
TiO_2	5.00	103.04 ± 6.46^{d}	92.07 ± 27.73	417.3 ± 31.1^{efg}	1.56 ± 0.28^{cde}	8.93 ± 0.83^{abc}
	10.00	126.32 ± 4.77^{ab}	104.18 ± 22.01	369.3 ± 45.0^{gh}	1.67 ± 0.46^{cde}	6.07 ± 0.50^{bc}
	15.00	124.61 ± 5.57^{ab}	115.18 ± 8.41	397.3 ± 22.0^{fgh}	1.95 ± 0.33^{abcde}	7.20 ± 1.22^{abc}
	20.00	124.93 ± 12.76^{ab}	104.70 ± 32.95	249.3 ± 10.1^{ij}	2.20 ± 0.38^{abc}	8.67 ± 1.29^{abc}

Anatomical, ultrastructural and cytological studies of *D. ferruginea* subsp. *ferruginea* L. exposed to nanoparticles

Ultrastructural and anatomical studies

In the TEM micrographs of the samples belonging to the control group, it is seen that the general structure and shape of the cell and the cell organelles are healthy and intact. Chloroplasts had well-compartmentalized grana and were regular in appearance, and their cell wall structures were intact (Fig. 3A, B). TEM data obtained from leaf samples treated with 1.25 µg/mL Cu NPs showed generally regular ultrastructural findings. The cell wall appeared orderly, and the chloroplasts were generally intact. However, thylakoid dissolutions were observed in a small number of chloroplasts. Mitochondrial structures were generally healthy (Fig. 4A). NP clusters were detected around a small number of damaged chloroplasts (Fig. 4B). In leaf samples treated with 7.5 µg/mL Cu NPs, it was observed that the cell wall thickened in some areas but maintained its integrity. In addition to starch grains, thylakoid dissolution was observed in the chloroplasts (Fig. 4C). Vacuole formations were also determined in some chloroplasts (Fig. 4D). In the TEM data obtained from leaf samples treated with 1.25 µg/mL CuO NPs, it was observed that the cell walls were emptied as a remarkable finding. NP accumulations were observed on the cell wall structures, in vacuoles and chloroplasts (Fig. 4E). Mitochondrial swellings and thylakoid dissolution in chloroplasts were observed in some regions (Fig. 4F). The data showed that the chloroplasts in the leaf samples treated with 7.5 µg/mL CuO NPs were generally well-organized, and plastoglobulin formations were present on the chloroplasts. However, it was observed that the cell wall structures were thickened and the inside was completely empty and white in color (Fig. 4G). NPs were observed in the vacuoles of the cells, along the cell wall and near the outer surfaces of the chloroplasts. Vacuolization was seen in some areas (Fig. 4H). At low concentrations (5 µg/mL) of Zn NPs, the integrity of the cell wall structure was preserved and NP clusters were found along the wall. Mitochondrial swelling, electron condensation in chloroplasts and thylakoid dissociation were observed in some regions (Fig. 5A). In this group, there was intense NPs accumulation along the cell wall and inside the vacuoles. Advanced damage and swelling were observed in

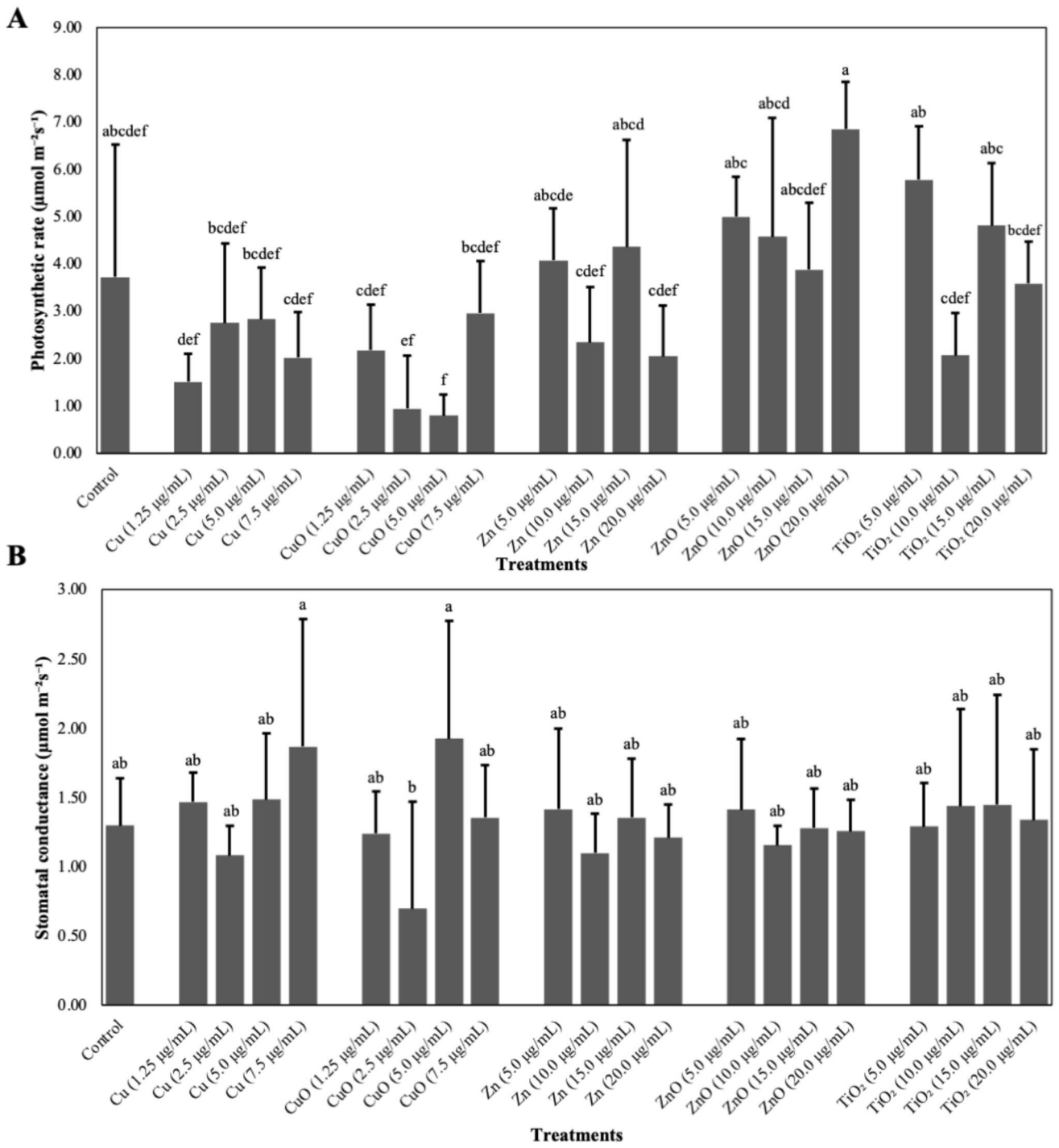

Fig. 2 **A** The differences in photosynthetic rates, **B** The differences in stomatal conductance

mitochondria (Fig. 5B). In groups treated with 20 µg/mL Zn NPs, although some chloroplast structures appeared healthy, some regions were completely fragmented and structural integrity was impaired. The surroundings of damaged chloroplasts were filled with NPs clumps. Cell wall structures were close to control (Fig. 5C). Mitochondrial swellings, cristae fractures and NPs clumps were detected in different regions within the cell (Fig. 5D). Common findings observed in groups treated with 5 µg/mL ZnO NPs include healthy chloroplast appearances with a well-organized thylakoid membrane and a high density of grana, plastoglobuli formations along with starch granules, and a particularly striking feature—NP clusters detected only in the samples treated with 5 µg/mL ZnO NPs, located within vacuole- or vesicle-like structures inside

Table 2 Impacts of nanoparticles on chlorophyll and carotenoid contents in *D. ferruginea* subsp. *ferruginea* L. leaves (Different superscript letters within a column represent significant differences according to one-way ANOVA followed by Tukey's test ($p \leq 0.05$). Groups without letters are not significantly different)

Treatments		Measurement parameters		
Nanoparticles (NPs)	Exposure concentration (µg/mL)	Chlorophyll a concentration (µg/mL)	Chlorophyll b concentration (µg/mL)	Carotenoid concentration (µg/mL)
Control (w/o) NPs	–	13.07 ± 2.86^{a}	5.72 ± 2.03^{ab}	2.65 ± 0.81^{ab}
Cu	1.25	9.75 ± 4.64^{abc}	4.68 ± 2.22^{ab}	3.17 ± 1.95^{a}
	2.50	11.33 ± 4.85^{abc}	5.88 ± 2.44^{ab}	2.33 ± 0.74^{ab}
	5.00	9.71 ± 3.43^{abc}	5.39 ± 2.18^{ab}	2.16 ± 0.87^{ab}
	7.50	6.80 ± 5.31^{bc}	3.72 ± 2.86^{ab}	2.00 ± 1.48^{ab}
CuO	1.25	10.53 ± 2.61^{abc}	4.86 ± 2.62^{ab}	2.06 ± 0.92^{ab}
	2.50	10.29 ± 3.18^{abc}	4.24 ± 1.36^{ab}	2.27 ± 0.79^{ab}
	5.00	10.44 ± 3.91^{abc}	4.56 ± 2.14^{ab}	2.05 ± 0.56^{ab}
	7.50	6.08 ± 4.14^{c}	2.45 ± 1.74^{b}	1.67 ± 1.15^{b}
Zn	5.00	11.32 ± 2.35^{abc}	5.04 ± 1.91^{ab}	2.52 ± 0.58^{ab}
	10.00	11.99 ± 3.02^{ab}	6.51 ± 3.70^{a}	2.60 ± 1.22^{ab}
	15.00	12.86 ± 4.10^{a}	6.23 ± 3.54^{a}	2.59 ± 0.92^{ab}
	20.00	12.83 ± 7.01^{a}	6.26 ± 4.95^{a}	2.40 ± 0.81^{ab}
ZnO	5.00	11.78 ± 3.60^{ab}	5.78 ± 3.18^{ab}	2.43 ± 0.83^{ab}
	10.00	12.04 ± 4.09^{ab}	5.53 ± 2.75^{ab}	2.46 ± 1.11^{ab}
	15.00	8.86 ± 2.92^{abc}	3.36 ± 1.74^{ab}	2.53 ± 1.14^{ab}
	20.00	11.61 ± 2.67^{ab}	5.39 ± 2.06^{ab}	2.56 ± 0.66^{ab}
TiO_2	5.00	12.94 ± 3.09^{a}	6.43 ± 2.99^{a}	2.71 ± 0.91^{ab}
	10.00	10.95 ± 2.78^{abc}	4.95 ± 2.28^{ab}	2.19 ± 0.67^{ab}
	15.00	12.89 ± 4.13^{a}	6.19 ± 3.30^{a}	2.37 ± 0.82^{ab}
	20.00	10.54 ± 3.35^{abc}	5.16 ± 2.95^{ab}	1.92 ± 0.59^{ab}

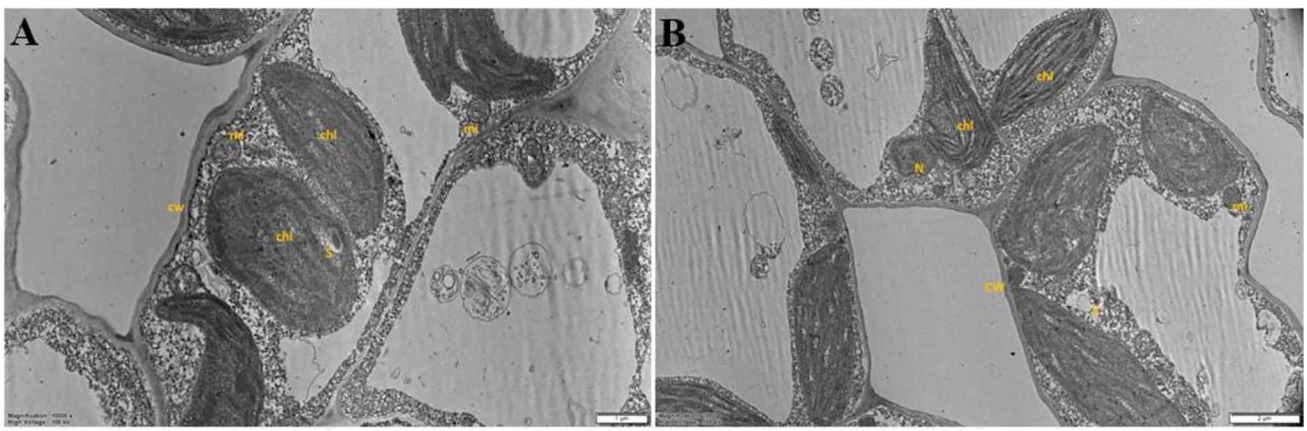

Fig. 3 TEM micrographs of control group leave cells of *Digitalis ferruginea* subsp. *ferruginea* L. plant (**A** = 1 µm and **B** = 2 µm scales). *cw* cell wall, *chl* chloroplast, *mi* mitochondria, *s* starch, *N* nucleus, *v* vacuole

the chloroplast (Fig. 5E). The cell walls appeared empty and NP clusters were detected around the chloroplasts (Fig. 5F). In contrast, the TEM findings of leaf samples treated with 20 µg/mL ZnO NPs predominantly displayed severely damaged ultrastructural characteristics. Cell wall structures were damaged, vacuolization increased, and thylakoid dissolution was observed in chloroplasts. NP clusters were observed in the chloroplasts and vacuoles (Fig. 5G, H). In leaf samples of *Digitalis ferruginea* subsp. *ferruginea* L. treated with 5 µg/mL TiO_2 NPs widespread ultrastructural findings included electron-dense appearances in some chloroplasts. However, chloroplast integrity and shapes were generally observed to be regular. Cell wall structures were healthy (Fig. 6A). Dense NPs accumulations were observed inside the vacuoles, along the cell wall and within the wall. Swelling was observed in mitochondria (Fig. 6B). The treatment with 20 µg/mL TiO_2

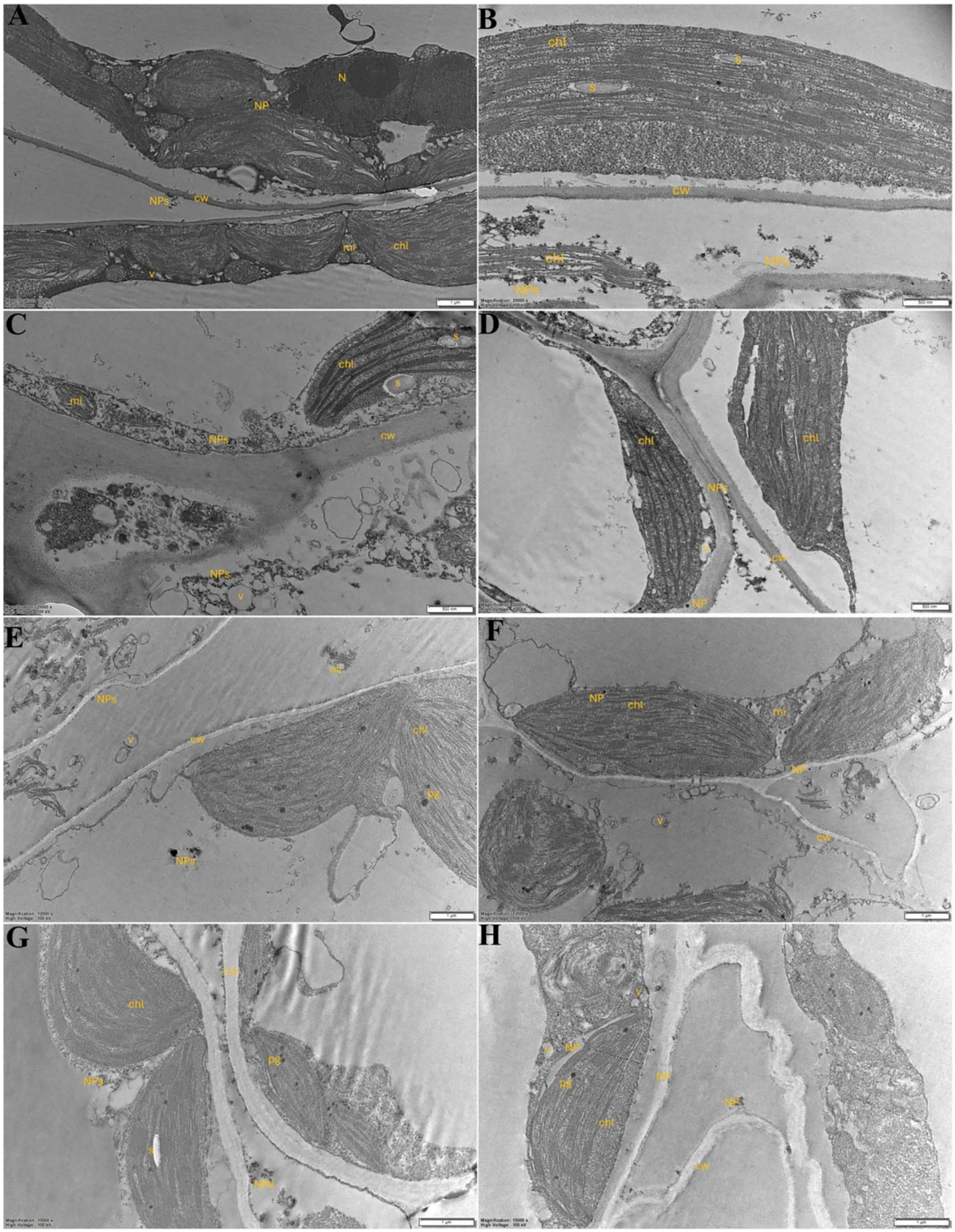
A
N
NP
NPs
cw
mi
chl
v
B
chl
S
S
cw
chl
NPs
NPs
C
S
chl
S
mi
NPs
cw
NPs
v
D
chl
chl
NPs
S
cw
NP
E
mi
NPs
v
cw
chl
pg
NPs
F
NP
chl
mi
NP
v
cw
G
cw
chl
pg
NPs
S
NPs
H
v
v
NP
pg
NP
NP
chl
cw

◂**Fig. 4** TEM micrographs of the *Digitalis ferruginea* subsp. *ferruginea* L. leaves treated with Cu NPs (**A** and **B**; 1.25 µg/mL- **C** and **D**); 7.5 µg/mL and CuO NPs (**E** and **F**; 1.25 µg/mL- **G** and **H**; 7.5 µg/mL). (**A**, **E**, **F**, **G**, **H** = 1 µm, **B**, **C**, **D** = 500 nm scales). *cw* cell wall, *chl* chloroplast, *mi* mitochondria, *s* starch, *N* nucleus, *v* vacuole, *NP* nanoparticle, *NPs* aggregate of nanoparticles, *pg* plastoglobuli

NPs, widespread ultrastructural findings generally included NP accumulations on the cell wall surface, within the cell wall, and sporadically in vacuoles. Severe mitochondrial damage, including swelling, membrane deformation, and cristae dissolution, was observed (Fig. 6C, D).

Cytological studies

The effects of NPs on the root tips of *D. ferruginea* subsp. *ferruginea* L. were examined for chromosomal aberration studies. Microscopic investigations indicated that some concentrations of NPs induced abnormalities in the cells, including issues such as anaphase and metaphase anomalies, chromosome breakage, spindle disturbances, fragmentation in chromosomes, sticky anaphases, and nuclear lesions (Fig. 7). The NPs increased the chromosomal abnormalities compared with the control. Exposure to Cu NPs (1.25, 2.50, and 7.50 µg/mL) caused sticky anaphase, nuclear lesions, and disruption of the metaphase (Fig. 7B–E). Conversely, CuO NPs (1.25, 2.50, 5.0, and 7.5 µg/mL) showed to induce chromosome mis-segregation, spindle disturbances, metaphase disruptions, anaphase bridges, and multiple nuclear lesions (Fig. 7F–I). Zn NPs did not cause any chromosomal abnormalities (Fig. 7J–M). 5.0 µg/mL of ZnO NPs led to chromosome breaks, and 10.0, 15.0, and 20.0 µg/mL caused fragmentation in chromosomes, anaphase bridge, and spindle disruptions (Fig. 7N–Q). Additionally, 5.0, 10.0, and 20.0 µg/mL of TiO_2 NPs affected metaphase formation, disrupted metaphase, and resulted in multiple nuclear lesions (Fig. 7R–U).

Nanoparticles' effects on root cell viability

A frequent technique for determining the root cell viability is to use Evans blue staining (Fig. 8). Differential uptake of the dye was detected in the roots of the plants exposed to NPs. When cell membrane integrity was evaluated by Evan's staining method, the highest damage was observed in CuO 2.50 µg/mL (0.049 ± 0.014) application ($p < 0.001$). ZnO 20.00 µg/mL (0.023 ± 0.004) had the lowest Evan's staining value and was one of the groups in which cell membrane integrity was best preserved (Fig. 9).

Discussion

This study presents the physiological, biochemical, and cytological responses of *D. ferruginea* subsp. *ferruginea* L. to different types and concentrations of Cu, CuO, Zn, ZnO, and TiO_2 NPs under in vitro conditions. The effects varied depending on particle type and dosage, ranging from responses to growth and cellular effects. Seed germinations were not significantly inhibited by NP treatments at the tested concentrations, although some variations were observed. For example, germination percentages were slightly reduced in Cu and Zn treatments at certain concentrations, whereas ZnO and TiO_2 groups showed rates closer to the control group. Previous studies have reported similar concentration-dependent effects, where low NP doses may have negligible or even positive effects, while higher doses can suppress germination (Rasheed et al. 2022; Aqeel et al. 2022; Gao et al. 2023). The impacts of NPs are related to their chemical properties, size, reactivity, and the specific plant species involved, potentially affecting nutrient absorption, photosynthetic characteristics, and growth (Rasheed et al. 2022). For example, CuO NP exposure in soybean and chickpea showed optimal growth at 100 and 60 µg/L, respectively, with inhibition beyond these limits (Adhikari et al. 2012). TiO_2 NPs have been shown to positively impact *Cicer arietinum* and forage crops like berseem and oat (Hajra and Mondal 2017; Maity et al. 2018), although some studies reported delayed germination at high doses (Ruffini Castiglione et al. 2011). These differences between our and previous results are likely due to the species-specific physiological and metabolic characteristics of *D. ferruginea* subsp. *ferruginea* L., the experimental conditions, and differences in the application protocol. These results suggest that TiO_2 NP–plant interactions are species- and condition-dependent.

Stomatal and trichome characteristics were significantly influenced by NP exposure. ZnO at 15.0 µg/mL increased stomatal density, suggesting potential stimulation of epidermal differentiation, while CuO at 2.5 µg/mL reduced trichome density. Changes in trichome and stomatal traits have been linked to plant adaptation strategies under stress, and previous study indicates that NPs can alter epidermal development by affecting hormonal balance and cell expansion (Da Costa and Sharma 2016; Wang et al. 2016).

Photosynthetic rate and stomatal conductance were also affected in a particle-specific manner. In our study, ZnO at 20.0 µg/mL resulted in the highest photosynthetic rate (6.85 ± 1.01 µmol $m^{-2} \cdot s^{-1}$), consistent with reports that Zn-based NPs can enhance gas exchange and photosynthetic efficiency (Kusumi et al. 2012). Conversely, CuO exposure markedly reduced both parameters (0.79 ± 0.45 µmol $m^{-2} \cdot s^{-1}$), in agreement with results of Cu-based NPs inducing oxidative stress and disrupting

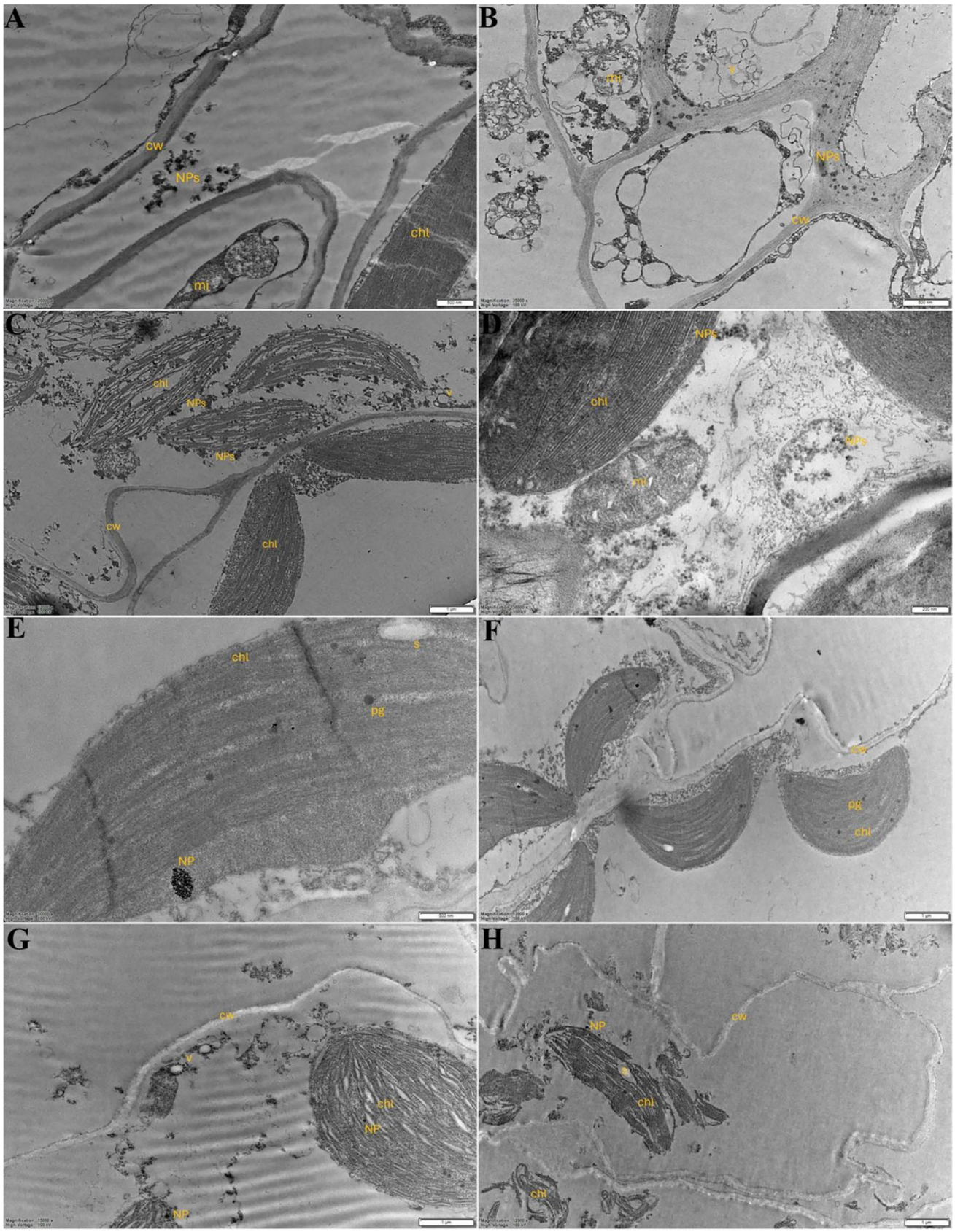
A
cw
NPs
chl
mi
B
mi
v
NPs
cw
C
chl
NPs
v
NPs
cw
chl
D
NPs
chl
NPs
mi
E
chl
s
pg
NP
F
cw
pg
chl
G
cw
v
chl
NP
NP
H
NP
cw
chl
chl

◂**Fig. 5** TEM micrographs of the *Digitalis ferruginea* subsp. *ferruginea* L. leaves treated with Zn NPs (**A** and **B**; 5 µg/mL- **C** and **D**; 20 µg/mL) and ZnO NPs (**E** and **F**; 5 µg/mL- **G** and **H**; 20 µg/mL). (**C**, **F**, **G**, **H** = 1 µm, **A**, **B**, **E** = 500 nm, **D** = 200 nm scales). *cw* cell wall, *chl* chloroplast, *mi* mitochondria, *s* starch, *N* nucleus, *v* vacuole, *NP* nanoparticle, *NPs* aggregate of nanoparticles, *pg* plastoglobuli

chloroplast function (Yang et al. 2020; Xiong et al. 2021). These contrasting effects underline the importance of NP composition and dosage in determining plant physiological responses.

Pigment content analysis revealed that CuO at 7.5 µg/mL reduced chlorophyll a and b levels, whereas Zn and TiO_2 treatments maintained pigment levels close to the control. Similar decreases in chlorophyll content due to CuO exposure have been observed in rice and barley (Shaw et al. 2014; Yang et al. 2020), possibly due to impaired chlorophyll biosynthesis or degradation of pigment-protein complexes under oxidative stress. In contrast, certain ZnO and TiO_2 treatments in other studies have been shown to maintain or enhance chlorophyll levels under stress conditions (Gohari et al. 2020).

Ultrastructural observations by TEM showed that low NP concentrations often preserved cell wall and chloroplast integrity, while higher concentrations caused thylakoid disorganization, mitochondrial swelling, and vacuolization. In controls, cell structures were robust. With 1.25 µg/L Cu NPs, thylakoids and grana were largely intact, with plastoglobuli observed in chloroplasts and NPs detected in the cell wall and vacuoles. ZnO at low doses showed well-structured chloroplasts with organized grana, whereas CuO and high ZnO treatments led to pronounced damage. CuO (7.5 µg/L) caused plastoglobule accumulation, consistent with *Landoltia punctata* under CuO NP stress (Rajput et al. 2018). ZnO at 5 µg/L also caused abnormalities, as reported in *Lolium perenne* and *Hordeum vulgare* (Lin and Xing 2008; Rajput et al. 2018, 2021).

Cytological analysis showed that CuO, TiO_2, and high-concentration ZnO treatments induced chromosomal abnormalities, such as anaphase bridges, spindle disturbances, and chromosome fragmentation. Similar toxic effects have also been reported in *Allium cepa* exposed to metal oxide NPs (Ahmed et al. 2018). The observed aberrations may result

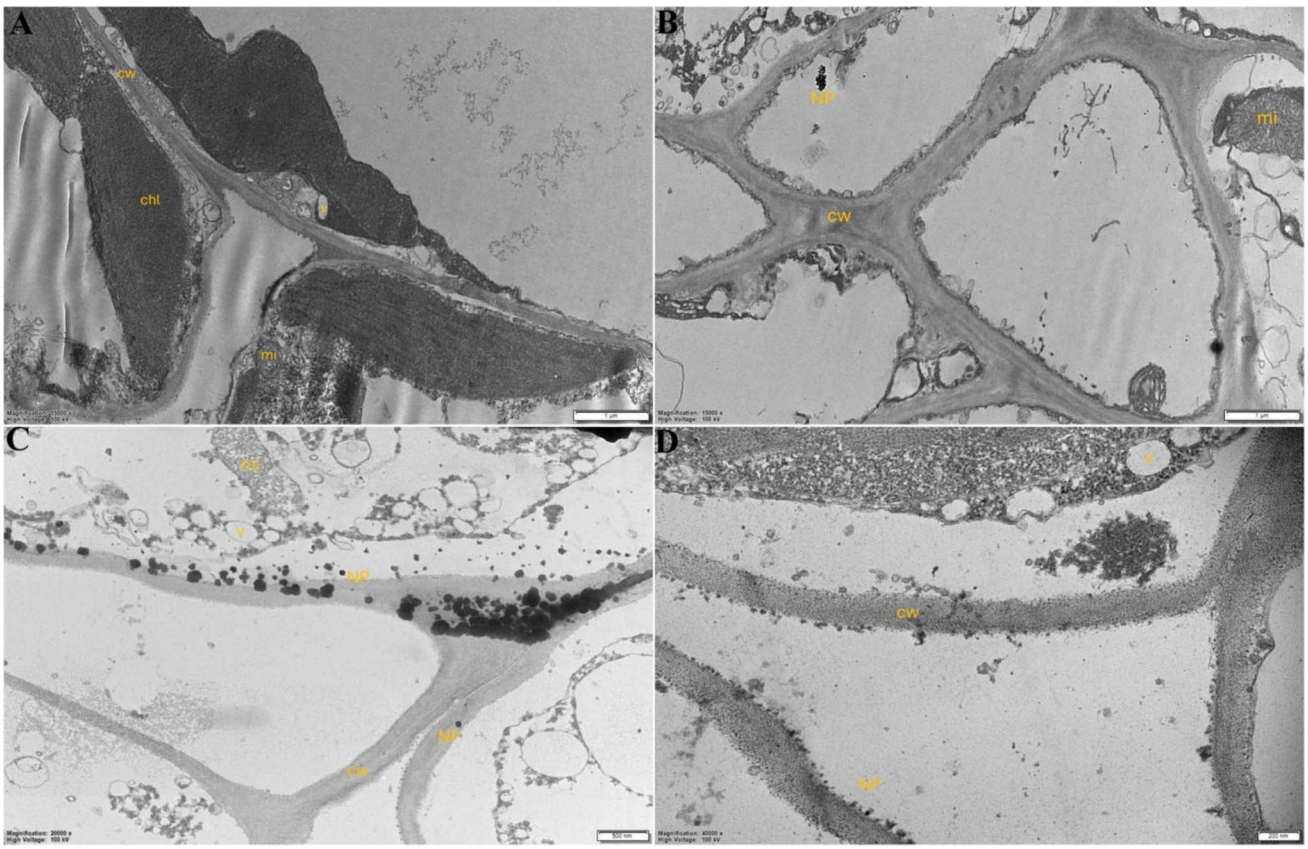

Fig. 6 TEM micrographs of the *Digitalis ferruginea* subsp. *ferruginea* L. leaves treated with TiO_2 NPs (**A** and **B**; 5 µg/mL- **C** and **D**; 20 µg/mL). (**A**, **B** = 1 µm, **C** = 500 nm, **D** = 200 nm scales). *cw* cell wall, *chl* chloroplast, *mi* mitochondria, *v* vacuole, *NP* nanoparticle, *NPs* aggregate of nanoparticles

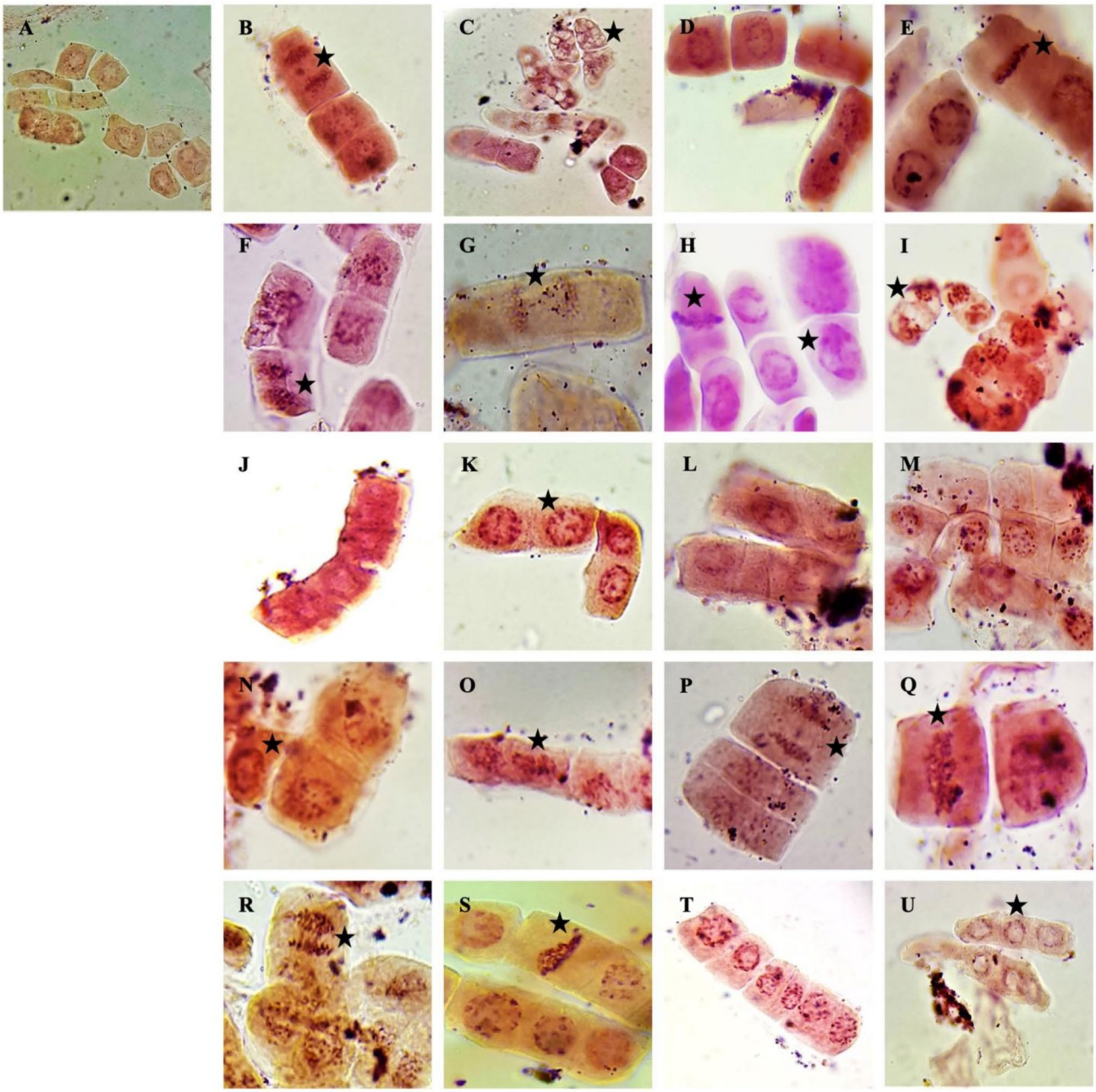

Fig. 7 Chromosomal abnormalities detected in the root meristematic cells of *D. ferruginea* subsp. *ferruginea* L. subjected to different doses of nanoparticles; **A** Control, **B** Cu 1.25 µg/mL, **C** Cu 2.5 µg/mL, **D** Cu 5.0 µg/mL, **E** Cu 7.5 µg/mL, **F** CuO 1.25 µg/mL, **G** CuO 2.5 µg/mL, **H** CuO 5.0 µg/mL, **I** CuO 7.5 µg/mL, **J** Zn 5.0 µg/mL, **K** Zn 10.0 µg/mL, **L** Zn 15.0 µg/mL, **M** Zn 20.0 µg/mL, **N** ZnO 5.0 µg/mL, **O** ZnO 10.0 µg/mL, **P** ZnO 15.0 µg/mL, **Q** ZnO 20.0 µg/mL, **R**TiO_2 5.0 µg/mL, **S** TiO_2 10.0 µg/mL, **T** TiO_2 15.0 µg/mL, **U** TiO_2 20.0 µg/mL. "★" indicates the Chromosomal abnormalities

from NP-induced interference with spindle apparatus function and DNA integrity.

Root cell viability assays by Evans blue staining showed that CuO at 2.5 µg/mL caused the highest membrane damage, whereas ZnO at 20.0 µg/mL maintained cell membrane integrity comparable to control. This aligns with studies indicating that Cu-based NPs are more likely to cause membrane lipid peroxidation (Shaw and Hossain 2013), while ZnO may exert less cytotoxicity at certain concentrations.

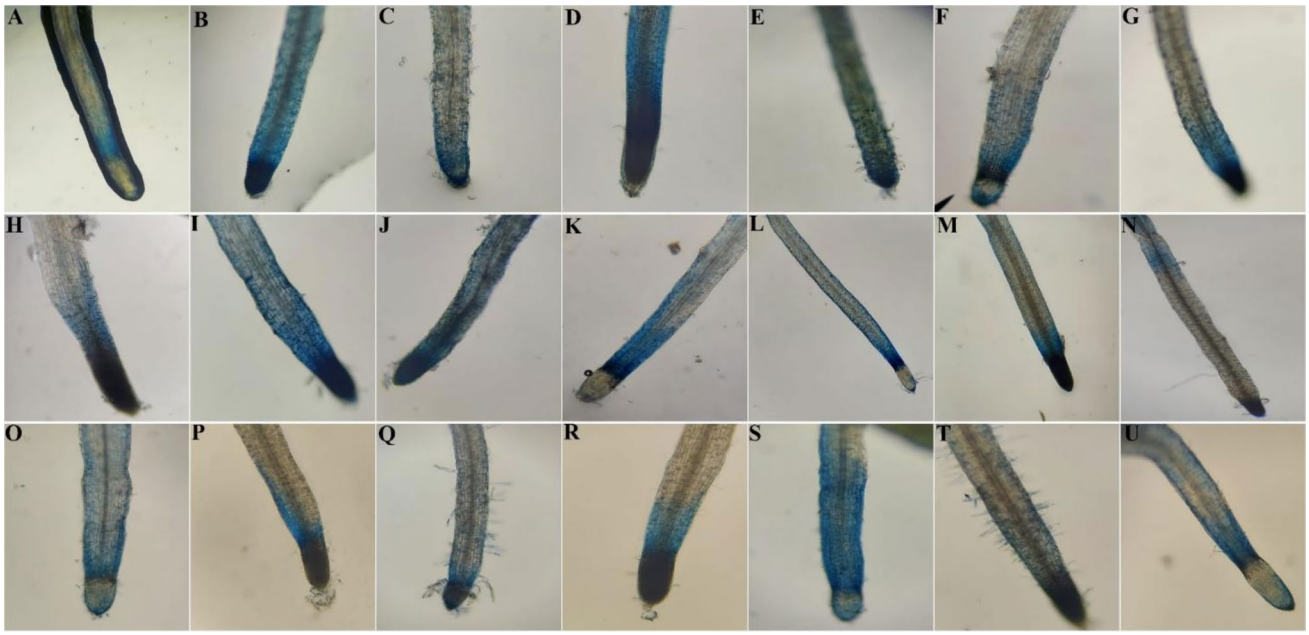

Fig. 8 Sample photographs from Evan's staining of the roots of *D. ferruginea* subsp. *ferruginea* L. subjected to different doses of nanoparticles. **A** Control, **B** Cu 1.25 µg/mL, **C** Cu 2.5 µg/mL, **D** Cu 5.0 µg/mL, **E** Cu 7.5 µg/mL, **F** CuO 1.25 µg/mL, **G** CuO 2.5 µg/mL, **H** CuO 5.0 µg/mL, **I** CuO 7.5 µg/mL, **J** Zn 5.0 µg/mL, **K** Zn 10.0 µg/mL, **L** Zn 15.0 µg/mL, **M** Zn 20.0 µg/mL, **N** ZnO 5.0 µg/mL, **O** ZnO 10.0 µg/mL, **P** ZnO 15.0 µg/mL, **Q** ZnO 20.0 µg/mL, **R** TiO_2 5.0 µg/mL, **S** TiO_2 10.0 µg/mL, **T** TiO_2 15.0 µg/mL, **U** TiO_2 20.0 µg/mL

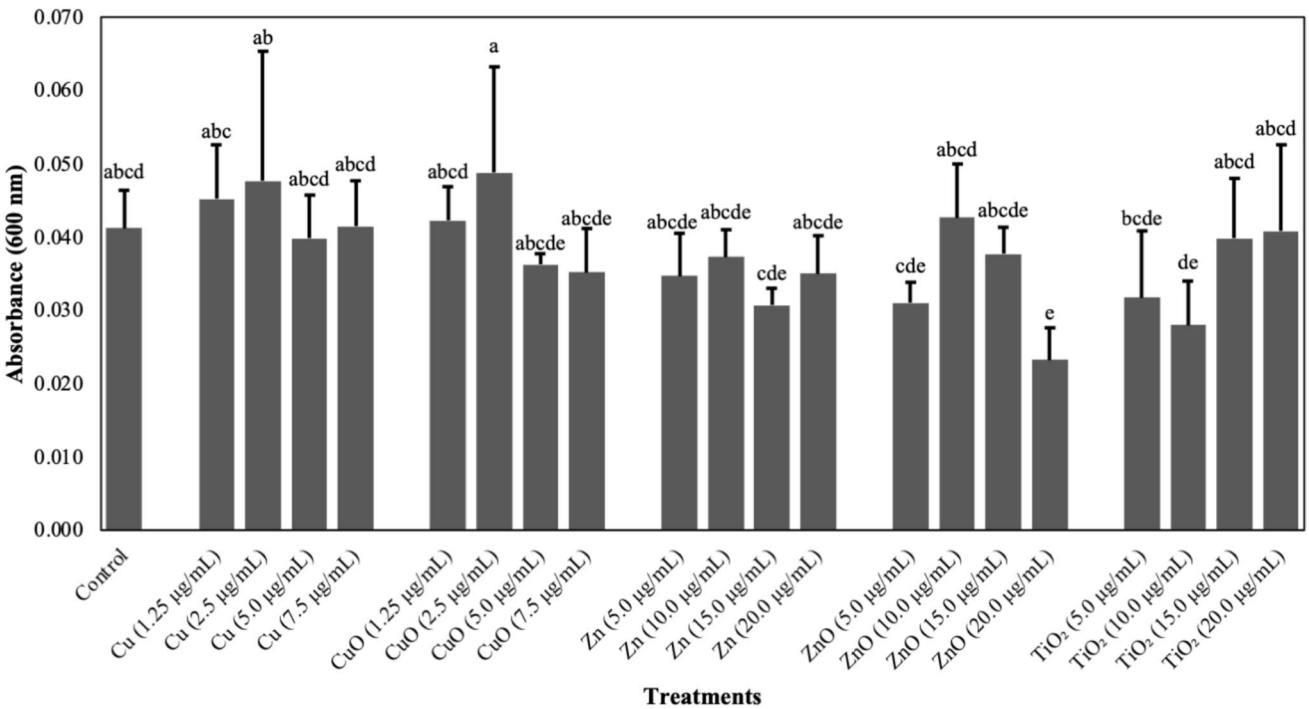

Fig. 9 Quantitative Evan's staining results

Overall, our results indicate that NP effects on *D. ferruginea* subsp. *ferruginea* L. are highly dependent on particle type and concentration. ZnO showed potential biostimulant effects at certain doses, increasing photosynthetic activity and maintaining cellular integrity, whereas CuO was consistently associated with negative impacts on pigment content, photosynthetic parameters, and cytological stability. The findings highlight the dual role of NPs as both growth promoters and stress inducers, emphasizing the need for careful selection of NP type and concentration in applications.

Conclusion

The study aimed to define the impacts of NPs at various concentrations on *D. ferruginea* subsp. *ferruginea* L., which is used as a medicinal plant. The effects were observed in seed germination, stomatal conductance and photosynthetic rate. Although NP exposure did not significantly inhibit germination, it was determined that it caused some biochemical and physiological changes. The study also assessed chlorophyll and carotenoid levels to reveal potential effects on photosynthetic pigments. In contrast to CuO NPs, which showed negative effects on chlorophyll contents and stomatal conductance, ZnO NPs caused an increase in photosynthetic rate. Molecular-level tests revealed genotoxic effects of NPs. Cellular damage was caused by NP accumulation, as indicated by ultrastructural studies, which occurred especially in vacuoles and chloroplasts. In plants exposed to CuO and TiO_2 NPs, abnormalities in chromosomes and decreased viability of root cells were noted. The findings highlight the fact that NPs function as biostimulants and possible stress sources for plants. These results highlight the need for controlled exposure levels to reduce the negative impacts of NPs. Moreover, it provides an opportunity to increase our knowledge of the complex processes that regulate plant responses to NPs exposure through the example of *D. ferruginea* subsp. *ferruginea* L. and provides a framework for further research and evaluation of plant health and ecological outcomes. In addition to all these results, the observed changes and effects indicate that *D. ferruginea* subsp. *ferruginea* L. may be a useful model for nanoparticle-plant interactions, especially for treatments where secondary metabolites are the focus of interest.

Supplementary Information The online version contains supplementary material available at https://doi.org/10.1007/s13205-025-04572-3.

Acknowledgements The authors would like to express their sincere gratitude to Ercan Selçuk Ünlü for providing access to laboratory facilities.

Author contributions Dipul Kumar Biswas: Methodology; Validation; Visualization; Writing—original draft; Writing—review and editing. Özge Kaya: Methodology; Validation; Writing—review and editing. Ömer Can Ünüvar: Methodology; Validation; Visualization; Writing—original draft; Writing—review and editing. Mehmet Örgeç: Methodology; Validation; Writing—review and editing. Sandeep Kumar Verma: Methodology; Validation; Writing—review and editing. İlknur Dağ: Methodology; Validation; Writing—review and editing. Mehmet Doğan: Methodology; Validation; Writing—review and editing. Buhara Yücesan: Methodology; Validation; Writing—review and editing. Muhammad Sameeullah: Methodology; Validation; Writing—review and editing. Songül Gürel: Methodology; Validation; Writing—review and editing. Ekrem Gürel: Methodology; Project administration; Supervision; Visualization; Writing—original draft; Writing—review and editing.

Funding This research was funded by the Scientific and Technological Research Council of Turkey (TÜBİTAK), Grant number 219Z161.

Data availability The datasets generated and analyzed during the current study are available from the corresponding author on reasonable request.

Declarations

Conflict of interest The authors declare that they have no conflict of interest.

References

Adhikari T, Kundu S, Biswas AK, Tarafdar JC, Rao AS (2012) Effect of copper oxide nano particle on seed germination of selected crops. J Agric Sci Technol A 2:815

Ahmed B, Shahid M, Khan MS, Musarrat J (2018) Chromosomal aberrations, cell suppression and oxidative stress generation induced by metal oxide nanoparticles in onion (*Allium cepa*) bulb. Metallomics 10:1315–1327. https://doi.org/10.1039/C8MT00093J

Aqeel U, Aftab T, Khan MMA, Naeem M, Khan MN (2022) A comprehensive review of impacts of diverse nanoparticles on growth, development and physiological adjustments in plants under changing environment. Chemosphere 291:132672. https://doi.org/10.1016/j.chemosphere.2021.132672

Asha A, Sivaranjani T, Thirunavukkarasu P, Asha S (2016) Green synthesis of silver nanoparticle from different plants—A review. Int J Pure Appl Biosci 4:118–124. https://doi.org/10.18782/2320-7051.2221

Baig N, Kammakakam I, Falath W (2021) Nanomaterials: a review of synthesis methods, properties, recent progress, and challenges. Mater Adv 2:1821–1871. https://doi.org/10.1039/D0MA00807A

Da Costa MVJ, Sharma PK (2016) Effect of copper oxide nanoparticles on growth, morphology, photosynthesis, and antioxidant response in *Oryza sativa*. Photosynthetica 54:110–119. https://doi.org/10.1007/s11099-015-0167-5

Davis PH, Mill RR, Tan K (1988) Flora of Turkey and The East Aegean Islands, (supplement), vol 10. Edinburgh University Press, Edinburgh

Eker I, Yücesan B, Sameeullah M, Welβ W, Müller-Uri F, Gürel E, Kreis W (2016) Phylogeny of Anatolian (Turkey) species in the *Digitalis* sect. *Globiflorae*(Plantaginaceae). Phytotaxa 244:263–282. https://doi.org/10.11646/phytotaxa.244.3.3

Gao M, Chang J, Wang Z, Zhang H, Wang T (2023) Advances in transport and toxicity of nanoparticles in plants. J Nanobiotechnol 21:75. https://doi.org/10.1186/s12951-023-01830-5

Gohari G, Mohammadi A, Akbari A, Panahirad S, Dadpour MR, Fotopoulos V, Kimura S (2020) Titanium dioxide nanoparticles (TiO_2 NPs) promote growth and ameliorate salinity stress effects on essential oil profile and biochemical attributes of *Dracocephalum moldavica*. Sci Rep 10:912. https://doi.org/10.1038/s41598-020-57794-1

Guzel Deger A, Çevik S, Kahraman O, Turunc E, Yakin A, Binzet R (2025) Effects of green and chemically synthesized ZnO nanoparticles on *Capsicum annuum* under drought stress. Acta Physiol Plant 47(2):17. https://doi.org/10.1007/s11738-025-03767-8

Hajra A, Mondal NK (2017) Effects of ZnO and TiO_2 nanoparticles on germination, biochemical and morphoanatomical attributes of *Cicer arietinum* L. Energy Ecol Environ 2:277–288. https://doi.org/10.1007/s40974-017-0059-6

Hülskamp M, Schwab B, Grini P, Schwarz H (2010) Transmission electron microscopy (TEM) of plant tissues. Cold Spring Harb Protoc. https://doi.org/10.1101/pdb.prot4958

Iwashita N (2016) Chapter 2—X-ray powder diffraction. In: Inagaki M, Kang F (eds) Materials science and engineering of carbon. Butterworth-Heinemann, Oxford, pp 7–25

Jacyn Baker C, Mock NM (1994) An improved method for monitoring cell death in cell suspension and leaf disc assays using evans blue. Plant Cell Tissue Organ Cult 39:7–12. https://doi.org/10.1007/BF00037585

Karale AN, Nigam B, Chaudhary IJ (2025) Impact of zinc oxide and titanium dioxide nanoparticles on growth parameters of chickpeas (*Cicer arietinum* L.). Explora: Environ Resour 0(0):025120024. https://doi.org/10.36922/EER025120024

Khan SH (2020) Green nanotechnology for the environment and sustainable development. Green materials for wastewater treatment. Springer, New York, pp 13–46

Kusumi K, Hirotsuka S, Kumamaru T, Iba K (2012) Increased leaf photosynthesis caused by elevated stomatal conductance in a rice mutant deficient in SLAC1, a guard cell anion channel protein. J Exp Bot 63:5635–5644. https://doi.org/10.1093/jxb/ers216

Lichtenthaler HK, Wellburn AR (1983) Determinations of total carotenoids and chlorophylls a and b of leaf extracts in different solvents. Biochem Soc Trans 11:591–592. https://doi.org/10.1042/bst0110591

Lin D, Xing B (2008) Root uptake and phytotoxicity of ZnO nanoparticles. Environ Sci Technol 42:5580–5585. https://doi.org/10.1021/es800422x

Ma S, Kabir G (1992) Interphase nuclear structure and heterochromatin in two species of *Corchorus* and their F1 hybrid. Cytologia 57:21–25. https://doi.org/10.1508/cytologia.57.21

Maity A, Natarajan N, Pastor M, Vijay D, Gupta CK, Wasnik VK (2018) Nanoparticles influence seed germination traits and seed pathogen infection rate in forage sorghum (*Sorghum bicolour*) and cowpea (*Vigna unguiculata*). Indian J Exp Biol 56:363–372

Murashige T, Skoog F (1962) A revised medium for rapid growth and bio assays with tobacco tissue cultures. Physiol Plant 15:473–497. https://doi.org/10.1111/j.1399-3054.1962.tb08052.x

Rajput V, Minkina T, Fedorenko A, Sushkova S, Mandzhieva S, Lysenko V, Duplii N, Fedorenko G, Dvadnenko K, Ghazaryan K (2018) Toxicity of copper oxide nanoparticles on spring barley (*Hordeum sativum distichum*). Sci Total Environ 645:1103–1113. https://doi.org/10.1016/j.scitotenv.2018.07.211

Rajput VD, Minkina T, Fedorenko A, Chernikova N, Hassan T, Mandzhieva S, Sushkova S, Lysenko V, Soldatov MA, Burachevskaya M (2021) Effects of zinc oxide nanoparticles on physiological and anatomical indices in spring barley tissues. Nanomaterials 11:1722. https://doi.org/10.3390/nano11071722

Rasheed A, Li H, Tahir MM, Mahmood A, Nawaz M, Shah AN, Aslam MT, Negm S, Moustafa M, Hassan MU, Wu Z (2022) The role of nanoparticles in plant biochemical, physiological, and molecular responses under drought stress: a review. Front Plant Sci 13:976179. https://doi.org/10.3389/fpls.2022.976179

Rastogi A, Zivcak M, Sytar O, Kalaji HM, He X, Mbarki S, Brestic M (2017) Impact of metal and metal oxide nanoparticles on plant: a critical review. Front Chem 5:78. https://doi.org/10.3389/fchem.2017.00078

Ruffini Castiglione M, Giorgetti L, Geri C, Cremonini R (2011) The effects of nano-TiO_2 on seed germination, development and mitosis of root tip cells of *Vicia narbonensis* L. and *Zea mays* L. J Nanopart Res 13:2443–2449. https://doi.org/10.1007/s11051-010-0135-8

Schneider CA, Rasband WS, Eliceiri KW (2012) NIH image to ImageJ: 25 years of image analysis. Nat Methods 9:671–675. https://doi.org/10.1038/nmeth.2089

Shaw AK, Hossain Z (2013) Impact of nano-CuO stress on rice (*Oryza sativa* L.) seedlings. Chemosphere 93:906–915. https://doi.org/10.1016/j.chemosphere.2013.05.044

Shaw AK, Ghosh S, Kalaji HM, Bosa K, Brestic M, Zivcak M, Hossain Z (2014) Nano-CuO stress induced modulation of antioxidative defense and photosynthetic performance of Syrian barley (*Hordeum vulgare* L.). Environ Exp Bot 102:37–47. https://doi.org/10.1016/j.envexpbot.2014.02.016

Stałanowska K, Szablińska-Piernik J, Okorski A, Lahuta LB (2023) Zinc oxide nanoparticles affect early seedlings' growth and polar metabolite profiles of pea (*Pisum sativum* L.) and wheat (*Triticum aestivum* L.). Int J Mol Sci 24(19):14992. https://doi.org/10.3390/ijms241914992

Tamás L, Šimonovičová M, Huttová J, Mistrík I (2004) Aluminium stimulated hydrogen peroxide production of germinating barley seeds. Environ Exp Bot 51:281–288. https://doi.org/10.1016/j.envexpbot.2003.11.007

Teske SS, Detweiler CS (2015) The biomechanisms of metal and metal-oxide nanoparticles' interactions with cells. Int J Environ Res Public Health 12:1112–1136. https://doi.org/10.3390/ijerph120201112

Verma SK, Sahin G, Yucesan B, Eker I, Sahbaz N, Gurel S, Gurel E (2012) Direct somatic embryogenesis from hypocotyl segments of *Digitalis trojana* Ivan and subsequent plant regeneration. Ind Crops Prod 40:76–80. https://doi.org/10.1016/j.indcrop.2012.02.034

Verma SK, Yucesan B, Sahin G, Gurel E (2014) Embryogenesis, plant regeneration and cardiac glycoside determination in *Digitalis ferruginea* subsp. *ferruginea* L. Plant Cell Tissue Organ Cult 119:625–634. https://doi.org/10.1007/s11240-014-0562-9

Verma SK, Das AK, Cingoz GS, Gurel E (2016) In vitro culture of *Digitalis* L. (foxglove) and the production of cardenolides: an up-to-date review. Ind Crops Prod 94:20–51. https://doi.org/10.1016/j.indcrop.2016.08.031

Verma SK, Das AK, Gantait S, Gurel S, Gurel E (2018a) Influence of auxin and its polar transport inhibitor on the development of somatic embryos in *Digitalis trojana*. 3 Biotech 8:99. https://doi.org/10.1007/s13205-018-1119-0

Verma SK, Gantait S, Jeong BR, Hwang SJ (2018b) Enhanced growth and cardenolides production in *Digitalis purpurea* under the influence of different LED exposures in the plant factory. Sci Rep 8:18009. https://doi.org/10.1038/s41598-018-36113-9

Vijayaraghavareddy P, Adhinarayanreddy V, Vemanna RS, Sreeman S, Makarla U (2017) Quantification of membrane damage/cell death using Evan's blue staining technique. Bio-Protoc. https://doi.org/10.21769/BioProtoc.2519

Wang P, Lombi E, Zhao F-J, Kopittke PM (2016) Nanotechnology: a new opportunity in plant sciences. Trends Plant Sci 21:699–712. https://doi.org/10.1016/j.tplants.2016.04.005

Willis AJ, Balasubramaniam S (1968) Stomatal behaviour in relation to rates of photosynthesis and transpiration in *Pelargonium*. New

Phytol 67:265–285. https://doi.org/10.1111/j.1469-8137.1968.tb06383.x

Xiong T, Zhang S, Kang Z, Zhang T, Li S (2021) Dose-dependent physiological and transcriptomic responses of lettuce (*Lactuca sativa* L.) to copper oxide nanoparticles—insights into the phytotoxicity mechanisms. Int J Mol Sci 22:3688. https://doi.org/10.3390/ijms22073688

Yamamoto Y, Kobayashi Y, Matsumoto H (2001) Lipid peroxidation is an early symptom triggered by aluminum, but not the primary cause of elongation inhibition in pea roots. Plant Physiol 125:199–208. https://doi.org/10.1104/pp.125.1.199

Yang Z, Xiao Y, Jiao T, Zhang Y, Chen J, Gao Y (2020) Effects of copper oxide nanoparticles on the growth of rice (*Oryza sativa* L.) seedlings and the relevant physiological responses. Int J Environ Res Public Health 17:1260. https://doi.org/10.3390/ijerph17041260

Yücesan B, Mohammed A, Eker İ, Sameeullah M, Demir-Ordu Ö, Cihangir C, Şahbaz N, Kaya Ö, Müller-Uri F, Kreis W, Gürel E (2016) In vitro propagation and cardenolide profiling of *Digitalis ferruginea* subsp. *Schischkinii*, a medicinally important foxglove species with limited distribution in Northern Turkey. In Vitro Cell Dev Biol-Plant 52:322–329. https://doi.org/10.1007/s11627-016-9759-4

Authors and Affiliations

Dipul Kumar Biswas[1,3] · Özge Kaya[3] · Ömer Can Ünüvar[3] · Mehmet Örgeç[3] · Sandeep Kumar Verma[1] · İlknur Dağ[4,5] · Mehmet Doğan[6] · Buhara Yücesan[7] · Muhammad Sameeullah[8,9] · Songül Gürel[2,3] · Ekrem Gürel[2,3]

✉ Ekrem Gürel
ekrem.gurel@igdir.edu.tr

Dipul Kumar Biswas
dipul.biswas@gmail.com

Özge Kaya
kaya_o@ibu.edu.tr

Ömer Can Ünüvar
omercanunuvar@hotmail.com

Mehmet Örgeç
mehmetorgec@gmail.com

Sandeep Kumar Verma
sandeep.20j@gmail.com

İlknur Dağ
ildag@ogu.edu.tr

Mehmet Doğan
mdogan@balikesir.edu.tr

Buhara Yücesan
buhara@ibu.edu.tr

Muhammad Sameeullah
sameepbg@gmail.com

Songül Gürel
songul.gurel@ibu.edu.tr

1 Institute of Sciences, SAGE University, Indore 452020, Madhya Pradesh, India

2 Faculty of Agriculture, Department of Agricultural Biotechnology, Iğdır University, Iğdır, Turkey

3 Faculty of Arts and Sciences, Department of Biology, Bolu Abant İzzet Baysal University, Bolu, Turkey

4 Central Research Laboratory Application and Research Center, Eskişehir Osmangazi University, Eskişehir, Turkey

5 Vocational Health Services High School, Eskisehir Osmangazi University, Eskisehir, Turkey

6 Faculty of Science and Literature, Department of Chemistry, Balıkesir University, Balıkesir, Turkey

7 Faculty of Agriculture, Department of Seed Science and Technology, Bolu Abant İzzet Baysal University, Bolu, Turkey

8 Faculty of Agriculture, Department of Field Crops, Bolu Abant İzzet Baysal University, Bolu, Turkey

9 Centre for Innovative Food Technologies Development, Application and Research, Bolu Abant Izzet Baysal University, Bolu, Turkey